ORIGINAL ARTICLE

http://dx.doi.org/10.5125/jkaoms.2016.42.1.20
pISSN 2234-7550 · eISSN 2234-5930

Investigation of a pre-clinical mandibular bone notch defect model in miniature pigs: clinical computed tomography, micro-computed tomography, and histological evaluation

Patricia L. Carlisle[1], Teja Guda[1,2], David T. Silliman[1], Wen Lien[1], Robert G. Hale[1], Pamela R. Brown Baer[1]

[1]Department of Craniomaxillofacial Regenerative Medicine, The United States Army Dental and Trauma Research Detachment, Fort Sam Houston, [2]Department of Biomedical Engineering, The University of Texas at San Antonio, San Antonio, TX, USA

Abstract (J Korean Assoc Oral Maxillofac Surg 2016;42:20-30)

Objectives: To validate a critical-size mandibular bone defect model in miniature pigs.

Materials and Methods: Bilateral notch defects were produced in the mandible of dentally mature miniature pigs. The right mandibular defect remained untreated while the left defect received an autograft. Bone healing was evaluated by computed tomography (CT) at 4 and 16 weeks, and by micro-CT and non-decalcified histology at 16 weeks.

Results: In both the untreated and autograft treated groups, mineralized tissue volume was reduced significantly at 4 weeks post-surgery, but was comparable to the pre-surgery levels after 16 weeks. After 16 weeks, CT analysis indicated that significantly greater bone was regenerated in the autograft treated defect than in the untreated defect (P=0.013). Regardless of the treatment, the cortical bone was superior to the defect remodeled over 16 weeks to compensate for the notch defect.

Conclusion: The presence of considerable bone healing in both treated and untreated groups suggests that this model is inadequate as a critical-size defect. Despite healing and adaptation, the original bone geometry and quality of the pre-injured mandible was not obtained. On the other hand, this model is justified for evaluating accelerated healing and mitigating the bone remodeling response, which are both important considerations for dental implant restorations.

Key words: Mandible, Autografts, Bone regeneration, Porcine, Critical-size defect

[paper submitted 2015. 10. 15 / revised 2015. 12. 22 / accepted 2015. 12. 29]

I. Introduction

Dental trauma and mandibular injuries generally occur as a result of violence, accidents, or battlefield engagements. These injuries affect a large number of Americans: in this country, craniofacial injuries make up more than 10% of all annual emergency room visits[1]. Furthermore, in recent conflicts in the Middle East, craniofacial injuries account for more than one-quarter of all injuries sustained by US soldiers[2,3]. A number of other situations can also lead to the need for mandibular reconstruction or augmentation; for example, periodontal disease, congenital defects, tumor resection of the mandible, and atrophy of the alveolar ridge due to tooth loss[4,5]. Often, mandibular reconstructions are complex and require multiple procedures[6]. To maximize the quality of life for these patients, the ideal outcome is to restore both proper mandibular form and function. Full restoration of mandible function includes the ability to eat normally; this often relies on the placement of dental implant restorations in proper occlusion.

For patients undergoing mandibular reconstruction, one significant challenge faced is that the bone does not heal to pre-injury volume; the height and/or width of the regenerated mandibular bone can be insufficient for implant restorations. Ideally, the implant should be encompassed by at least 1 mm of alveolar bone in order to properly support the prosthesis[7]. In addition to bone quantity, bone quality is an essential com-

Teja Guda
Department of Biomedical Engineering, The University of Texas at San Antonio, One UTSA Circle, AET 1.356, San Antonio, TX 78249, USA
TEL: +1-210-458-8529 FAX: +1-210-458-7007
E-mail: teja.guda@utsa.edu
ORCID: http://orcid.org/0000-0002-3218-2916

ponent contributing to implant success[8]. Many bone regenerative therapies are available to treat mandibular injuries and augment alveolar ridges. Unfortunately, none of these treatments are reliable enough to be considered the single clinical gold-standard[5,9,10]. In order to develop improved therapies for craniofacial bone regeneration, it is important to gain a better understanding of the mechanisms involved in the healing process.

To ensure safety and efficacy of novel craniofacial-specific biomaterials, they are often initially tested in small animal calvarial models. Prior to clinical trials, promising materials are often tested for anatomically appropriate efficacy in a larger pre-clinical animal model with comparable mandibular size and dentition to humans. Testing therapies in these relevant models allows us to be more confident that findings will be clinically translatable. Furthermore, by standardizing the large animal models used across the field, results from numerous studies can be easily compared. Researchers have historically used dogs, goats, sheep, or pigs as a large animal model to perform pre-clinical craniomaxillofacial (CMF) bone healing trials; with each model having specific advantages and drawbacks[11].

Goats[12-14] and sheep[15-19] have been used in numerous studies to further the understanding of craniofacial bone healing. However, the dentition of these animals is characterized by elongated tooth roots, continuously erupting teeth, and herbivorous chewing pattern, which are quite different from humans. Dogs have been used extensively to study bone healing in mandibular defects, including the use of notch-type defects at the inferior margin[20-22]. Dogs have similar dentition to humans and are considered a good model to study maxillofacial bone healing[23]. Even so, they can be expensive; especially when breed-matched studies are performed. Furthermore, ethical concerns regarding the use of companion animals in medical research have prompted many groups to seek alternative models[11]. The pig is an attractive model because its mandible closely resembles the human mandible with regard to anatomy, morphology, healing, bone composition, bone remodeling and dentition[24,25].

Mandibular defect models in pigs are used to evaluate the efficacy of promising new biomaterials[26]; however, some inconsistency has been noted in the literature as to the size of the defect that defines a critical-sized defect (CSD) in these models. The non-segmental bone notch defect model is one such pig model that is useful in evaluating bone healing due to the fact that it mimics localized edentulous bone atrophy. A number of studies have selected a 5 cm^3 defect as the CSD to evaluate bone healing potential of various therapies[27,28]. However, a subsequent report suggests that a 5 cm^3 defect may not be stringent enough to be defined as a CSD. That study found that, with the creation of a resected bone block (~10.1 cm^3) in the anterior alveolar region with periosteal preservation, the defect showed spontaneous regeneration via a normal physiologic response[29]. Ma et al.[30] demonstrated that segmental defects as large as 6 cm in length in the presence of the periosteum or 2 cm in length when the periosteum was resected could be considered CSDs in the pig mandible. These results provide further support for the idea that the periosteum plays a key role in bone regeneration in large defects.

There is a significant need to develop bone regenerative therapies to restore mandibular and craniofacial defects in a predictable manner. As such, it is essential that our preclinical models are appropriate and stringent for testing these novel therapies so that we have confidence in our study results. Due to the inconsistencies in the available literature regarding the definition and characterization of CSD healing in the miniature pig mandibular defect model, further investigation of a non-healing notch defect is necessary. In the current study, we sought to define healing in a surgically-created mandibular notch defect measuring a minimum of 3×2×1 cm^3 (volume=6 cm^3) with adjacent periosteal stripping in Sinclair miniature pigs. We hypothesized that this model would mimic a similar human mandibular injury and would not heal without intervention. Upon defining this model as a CSD model, studies can then move forward to test promising bone regenerative therapeutics in the CMF region and justify their translation for use in human clinical studies.

II. Materials and Methods

1. Experimental design

To evaluate the healing potential in mandibular bone defects, either with no restoration (negative control) or with autologous bone graft restoration (clinical standard), notch defects $\geq$6 cm^3 in volume were created bilaterally in five dentally-mature Sinclair miniature pigs (>1 year of age). Bone healing was monitored for 16 weeks; *in vivo* radiographic assessments were performed prior to surgery, 4 weeks post-surgery, and 16 weeks post-surgery. This research study was approved by the Institutional Animal Care and Use Committee at the United States Army Institute of Surgical Research (No. A-11-017). A schematic representation of the

surgical protocol is shown in Fig. 1. A.

2. Clinical procedures

Bilateral mandible defects were created using an extra-oral surgical approach; specifically, the defects were anatomically located anterior to the antegonial notch and posterior to the mental foramen. Approximately 24 hours prior to surgery, a fentanyl transdermal patch (100 μg/hr) was applied to ensure appropriate levels of peri- and post-surgery analgesia. Thirty minutes prior to surgery, Telazol (4.4 mg/kg intramuscular; Zoetis, Florham Park, NJ, USA) was administered as anesthetic induction. Isoflurane (1.5%-4.0%) and oxygen were then used to maintain anesthesia. Following anesthetic induction, prophylactic antibiotics (cefazolin, 1 g) were administered, and the surgery site was prepared to ensure sterility. A skin incision was made parallel to the inferior border on both sides of the mandible, and the skin was reflected. Using a reciprocating bone saw cooled with copious sterile saline, right and left mandibular osseous defects were created, followed by proximal periosteum dissection.(Fig. 1. B, 1. C) These defects were approximately 6 cm^3 in volume (anterior-posterior=3 cm, buccal-lingual=1 cm, inferior border-height of contour=2 cm).(Fig. 1. D-F) To aid in histological analysis, gutta-percha was placed into small holes created in the cortical bone at the defect borders. Bone sectioned from each side was ground in the R. Quétin Bone-Mill (Quétin Dental-Products, Leimen, Germany) to morselize both the cortical and cancellous bone.(Fig. 1. G, 1. H) The morselized bone from both sides was combined, hydrated with sterile saline,

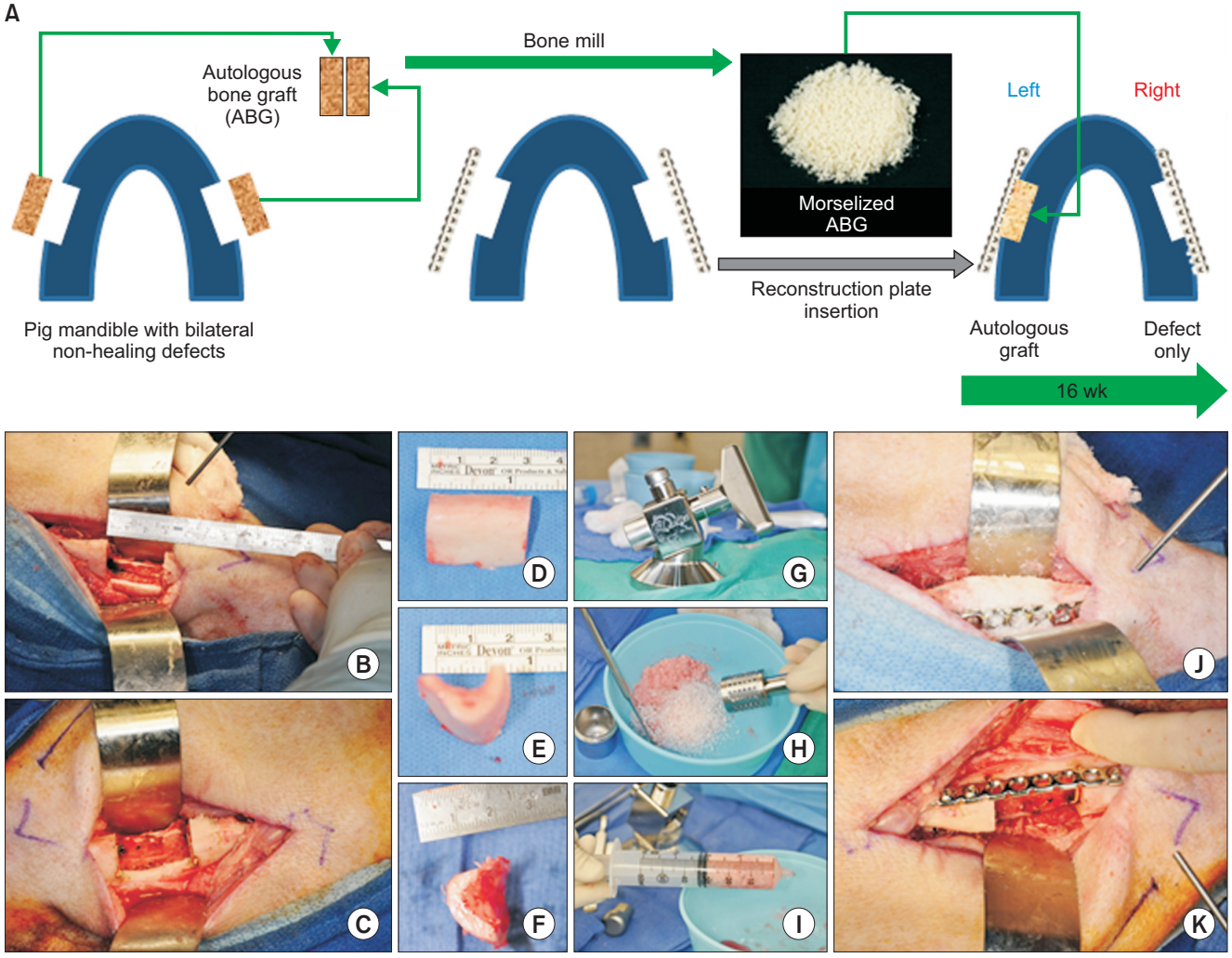

Fig. 1. A. Schematic diagram of the mandibular bone notch defect study design. B, C. Surgical images of the bilateral bone defects in pigs (n=5). The removed bone (D-F) was morselized, hydrated with sterile saline (G-I) and packed into the left side defect, serving as autograft (J), whereas the right side received no treatment (K); both hemi-mandibles were fixed with plates.
Patricia L. Carlisle et al: Investigation of a pre-clinical mandibular bone notch defect model in miniature pigs: clinical computed tomography, micro-computed tomography, and histological evaluation. J Korean Assoc Oral Maxillofac Surg 2016

compressed (Fig. 1. I), and placed to fill the left side of the mandibular defect.(Fig. 1. J) A small amount of morselized bone was reserved for scanning electron microscopy evaluation of particle size. The right side defect remained untreated. (Fig. 1. K) All defects were plated using a 2.7 mm reconstruction plate with 2.7 mm self-tapping cortex screws (Synthes Vet, West Chester, PA, USA).(Fig. 1. J, 1. K) Prior to reapproximating the tissue layers with resorbable 3-0 Vicryl sutures (Ethicon US LLC, Somerville, NJ, USA), a Jackson-Pratt drain was placed into the surgical wound site. The drain was removed 24 to 48 hours post-surgery. Next, 64-slice computed tomography (CT) scans (Aquilion 64 Multislice Helical CT Scanner; Toshiba American Medical, Tustin, CA, USA) were performed under anesthesia (following the above described anesthesia protocol) immediately prior to surgery and 4 and 16 weeks post-surgery. Following the 16 week final CT scan, the pigs were euthanized via intravenously administered Fatal-Plus (1 mL/4.5 kg; Vortech Pharmaceuticals, Dearborn, MI, USA).

3. Sixty-four slice computed tomography

Sixty-four slice CT scan images were acquired at an effective pixel size of 500 μm, and three-dimensional rendering of the image sets was performed using a standard "bone mask" in Vitrea Core (version 6.3; ViTAL, Minnetonka, MN, USA). The clinical volumes were then upsampled using tri-linear interpolation at a factor of 5 (ImageJ version 1.47; National Institutes of Health, Bethesda, MD, USA) so that the resolution was 100 μm[31]. DataViewer (SkyScan, Kontich, Belgium) was used to re-align the mandibles along the physiological axes, and dentition landmarks were used to ensure that the scans at different time points were all aligned in an identical fashion. The image stack was then imported into CTAn software version 1.11 (SkyScan), and a region of interest (ROI) was created to cover the defect site. The region was defined by the contour of the intact bone from the pre-surgical scan and was fixed within each animal for evaluation at 4 and 16 weeks.(Fig. 2. A) The defect site ROI spanned an average of 3 cm long, 1 cm deep, and 2 cm wide (full thickness). A threshold of 659 mgHA/mL was selected across all samples using the Otsu algorithm[32] to distinguish mineralized tissue from unmineralized tissue within the defect. A secondary ROI was defined over the same length in each pig to evaluate any changes in bone morphology above the notch (intact bone excluding teeth, as outlined with a dashed line in Fig. 3. A). The bone volume fraction and bone mineral density of the mineralized tissue were calculated within each ROI for each sample using CTAn.

4. Micro-computed tomography

After the 16 week harvest, the mandibles were hydrated with formalin, and micro-computed tomography (μCT) analysis was performed using a SkyScan 1072 scanner (Bruker MicroCT, Kontich, Belgium) at a resolution of 36 μm/pixel.

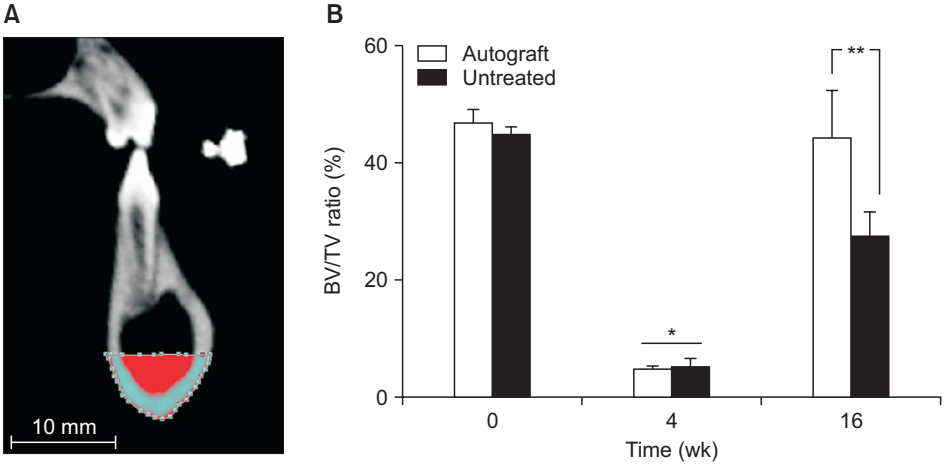

Fig. 2. Computed tomography (CT) quantification of regenerated bone over the healing time course. A. Using a single slice axial view of the 64-slice CT of the mandible, the bone defect region of interest (outlined by a dotted border) was defined. B. Bone volume/tissue volume (BV/TV) ratio was calculated for all time points in the autograft-treated and untreated sides in each pig (n=5). *Significant differences between weeks at the same time point (P<0.001). **Significant differences between groups at the same time point (P=0.013).

Patricia L. Carlisle et al: Investigation of a pre-clinical mandibular bone notch defect model in miniature pigs: clinical computed tomography, micro-computed tomography, and histological evaluation. J Korean Assoc Oral Maxillofac Surg 2016

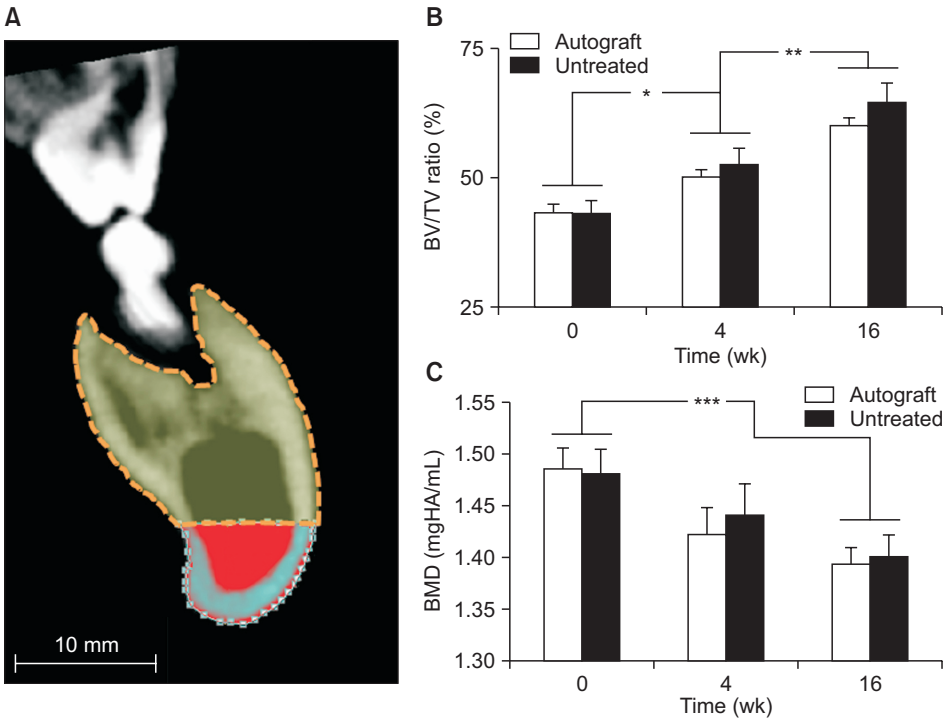

Fig. 3. Computed tomography quantification of bone superior to the intact mandible over the healing time course. A. The region of interest (outlined by a dashed border) was defined to include the intact bone above the defect (shaded by horizontal lines) and exclude the teeth. Bone volume/tissue volume (BV/TV) ratio (B) and bone mineral density (BMD) (C) was calculated for all time points in the autograft-treated and untreated sides in each pig (n=5). Significant differences indicated by $^{*}P$=0.013, $^{**}P$<0.001, $^{***}P$=0.005.
Patricia L. Carlisle et al: Investigation of a preclinical mandibular bone notch defect model in miniature pigs: clinical computed tomography, micro-computed tomography, and histological evaluation. J Korean Assoc Oral Maxillofac Surg 2016

The images were reconstructed using NRecon software (Bruker MicroCT) to generate grayscale images. DataViewer was used to re-align the mandible images using dentition landmark registration to the 64-slice CT data for consistency. A uniform threshold for bone was determined across all samples using the Otsu algorithm and the bone defect ROIs. Bone volume to total volume ratio was determined on the μCT images using CTAn.

5. Histology

The excised mandible sections were prepared for histology by dehydration in ascending concentrations of ethanol, followed by xylene at 4°C and then embedding in poly(methyl methacrylate). The specimens were then cut and ground to 30-μm thick sections using a diamond saw and MicroGrinder (Exakt Technologies, Oklahoma City, OK, USA). The sections were mounted on slides, stained with Sanderson's rapid bone stain, then counterstained with van Gieson's picrofuchsin to stain soft tissue blue and stain bone pink/red. Next, 2.0× magnification histology slide images were acquired on an Olympus SZX16 research high-class stereo microscope (Olympus, Center Valley, PA, USA) with an Olympus DP71 microscope digital camera and compiled using Photoshop (version 7.0.1; Adobe Systems Inc., San Jose, CA, USA). High magnification images (40× and 100×) were acquired on a Nikon Eclipse 55i research microscope with a DS-f11 digital camera (Nikon Instruments Inc., Melville, NY, USA).

6. Statistical analysis

All data are represented as mean±standard error of the mean. Significance in 64-slice CT measures was determined using a two-way ANOVA (across time and experimental group) and Tukey's test for post-hoc evaluation when significance was found (SigmaPlot version 11.0; Systat Software Inc., San Jose, CA, USA). In the case of the μCT data, a paired t-test analysis was used to determine significant difference. The significance level was set at P<0.05 for all statistical measures. Correlation between 64-slice CT and μCT data was determined by linear regression analysis.

III. Results

1. Animal model

In order to evaluate the healing potential of a defined mandibular bone notch defect, we introduced a 7.5 cm^3 notch (average size as determined by CT analysis) on each side of the mandible in each of 5 dentally mature Sinclair miniature pigs. The bone removed during both the right and the left defect creations was morselized, combined, and then placed into the left side defect, serving as autograft. The average size of the morselized particles was found to be 670 μm by scan-

ning electron microscopy analysis. Bone healing in the pigs was assessed at 4 weeks post-surgery via CT scans and at 16 weeks post-surgery using CT, μCT, and histological techniques.

2. Sixty-four slice computed tomography analysis

The use of clinical CT scans allowed us to monitor bone healing throughout the course of the experiment and compare bone regeneration at multiple time points. Sixty-four slice CT scans were taken at 3 time points: immediately before the defect creation, at 4 weeks post-surgery, and at 16 weeks post-surgery. The bone volume to tissue volume (BV/TV) ratio was calculated within the defect ROI.(Fig. 2. A; outlined in dotted line) At 4 weeks post-surgery, measurement of bone volume based on CT scan data revealed an absence of mineralized tissue within both the autograft-treated (180.7±46.5 mm^3) and untreated defect sites (265.3±111.7 mm^3) in all pigs. In both defect sites at 4 weeks, measurement of the BV/TV ratio showed significantly less bone volume compared to both the pre-surgery and 16 weeks post-surgery time points (P<0.001).(Fig. 2. B)

At 16 weeks post-surgery, bone volume measurements showed substantial bone regeneration in both defects: The mean bone volume measured 2,487.2±507.8 mm^3 in the autograft-treated defect sites and 1,665.0±335.7 mm^3 in the untreated defect sites. Moreover, in both sites, bone volume was approaching pre-surgical bone volume value (2,114.1± 175.9 mm^3). Irrespective of treatment, no significant intra-group differences in bone volume were found between pre-surgery and 16 weeks post-surgery time points. However, at 16 weeks, significantly higher bone volume was regenerated in the autograft-treated defects compared with the untreated defects (P=0.013).(Fig. 2. B) These same trends in bone regeneration were observed in three-dimensional reconstructions of each hemi-mandible from a representative animal. (Fig. 4)

3. Micro-computed tomography analysis

For the purpose of obtaining higher resolution data regarding the bone healing in this model, μCT imaging was used to analyze BV/TV ratio in the defect space post-mortem. Representative axial and longitudinal cross-sectional μCT images are pictured in Fig. 5. A. In the images of both the autograft-treated and untreated groups, significant bone growth was evident in the defect space. The superior margins of the defect were identifiable by white gutta-percha markers (indicated

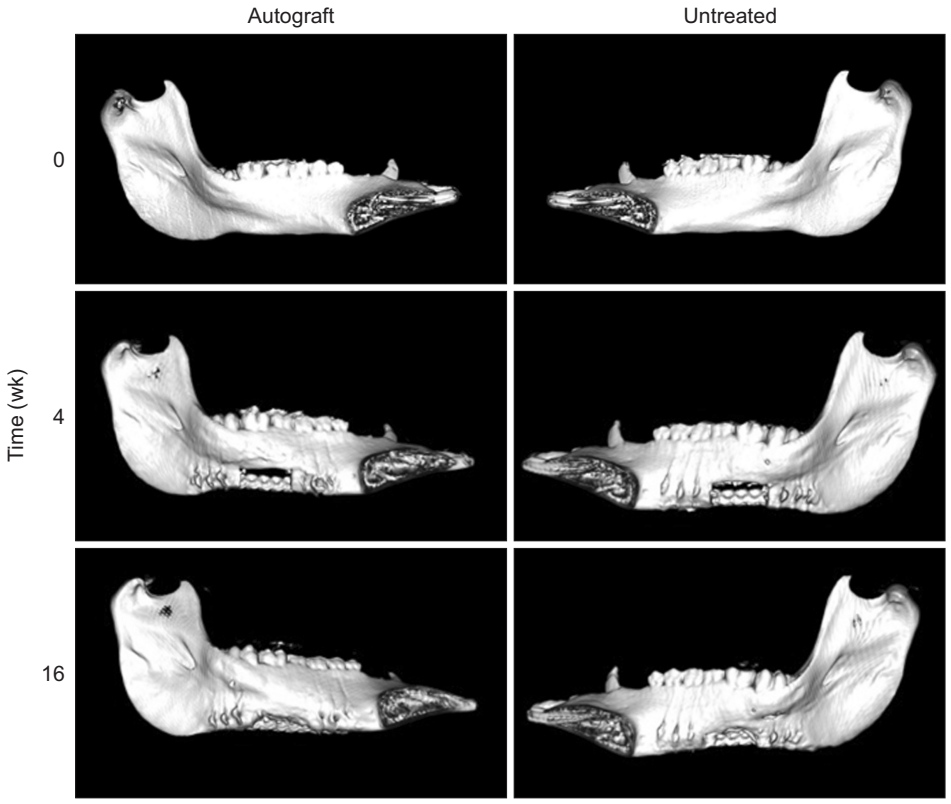

Fig. 4. Lingual view of three-dimensional reconstructions of hemi-mandibles from 64-slice computed tomography images. Volumetric rendering of mineralized tissue and fixation plates of the autograft-treated (left panels) and untreated (right panels) mandibles from one pig at 0 weeks (pre-surgery), 4 weeks post-surgery and 16 weeks post-surgery to represent the pattern of bone regeneration at each time point.
Patricia L. Carlisle et al: Investigation of a pre-clinical mandibular bone notch defect model in miniature pigs: clinical computed tomography, micro-computed tomography, and histological evaluation. J Korean Assoc Oral Maxillofac Surg 2016

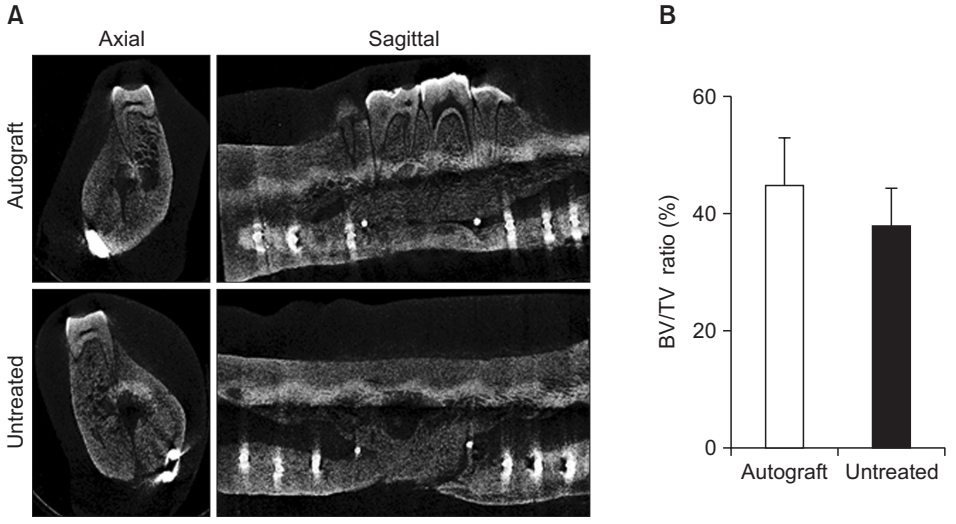

Fig. 5. Quantification of bone regeneration by micro-computed tomography (μCT) analysis. A. High resolution μCT was performed post-mortem on both the autograft-treated and untreated sides of the mandible for each pig (n=5). A representative axial cross-section (left panels) and sagittal cross-section (right panels) are shown here for both the autograft-treated (upper) and untreated (lower) sides. Gutta-percha denotes the defect margins (designated by the two centermost single white dots in the sagittal cross-sections). B. Bone regeneration was quantified and reported as the bone volume/tissue volume (BV/TV) ratio (P=0.46).
Patricia L. Carlisle et al: Investigation of a pre-clinical mandibular bone notch defect model in miniature pigs: clinical computed tomography, micro-computed tomography, and histological evaluation. J Korean Assoc Oral Maxillofac Surg 2016

by the two centermost single white dots). Qualitatively, these images show little difference in bone healing between treatment groups. Greater bone regeneration was seen at the posterior interface compared to the anterior interface of the notch in both groups; this result was observed in all 5 pigs. Quantification of the BV/TV ratio indicated that there was no significant difference between the autograft-treated and the untreated groups; however, similar to the CT results, more bone was regenerated in the autograft-treated defect compared to the non-treated defect (P=0.46).(Fig. 5. B) Furthermore, the results of the μCT analysis were consistent with the clinical CT analysis in demonstrating significant bone volume regeneration in both the treated and untreated defect spaces. A high correlation exists between the CT and μCT results (R^2=0.83).

4. Histological analysis

In order to detect calcified bone, fibrous tissue formation, and the presence of cellular activity, histological analysis was performed on the regenerated mandibular bone. For both the treated and untreated defects, the histological slides revealed intramembranous trabecular-like healing into the defect from the anterior, posterior, and superior walls.(Fig. 6) In general, the autograft-treated defects had a greater extent of thin trabecular spindles penetrating deep into the defect space. The non-treated defects showed less bony invasion into the defect space; however, the trabecular-like in-growth was observed to occur in dense bone fronts.(Fig. 6) In all pigs, neither defect spaces contain healed dense bone bridging of the inferior cortex or restoration of the bony anatomy to its pre-surgical condition.

5. Bone adaptation analysis

During the histological analysis process, we noted significant bone regeneration in the marrow space, superior to the initial defect. This observation led to the further investigation of the bone remodeling adjacent to the defect sites. First, analysis of the 64-slice CT scans was performed using an alternate ROI encompassing intact bone.(Fig. 3. A; outlined in dashed lines) Compared to pre-surgery values, the ROI superior to the surgical site had a significant increase in bone volume fraction at 4 weeks post-surgery (P=0.013).(Fig. 3. B) At 16 weeks post-surgery, there was a further significant increase in bone volume in the superior site (P<0.001). However, the increase in bone volume in this superior ROI was associated with a decrease in bone mineral density: These values were significantly lower after 16 weeks compared to preoperative levels (P=0.005).(Fig. 3. C) Together, these results suggest that the bone did in fact remodel to increase load-bearing ability and compensate for the lack of bone in the defect area. These results were consistent between treat-

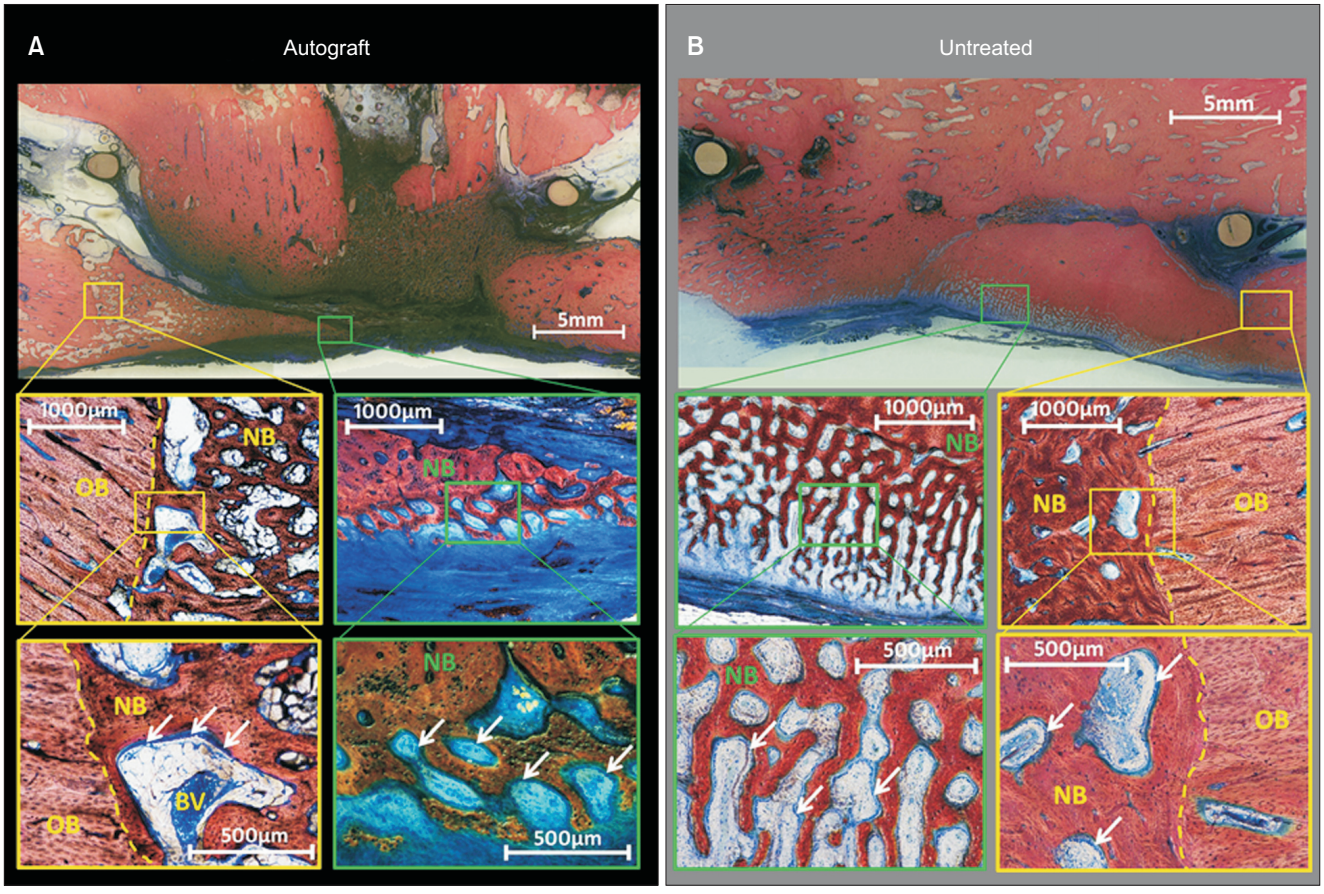

Fig. 6. Histological sections along the sagittal cross-section of the mandible. The autograft-treated (A) and the corresponding untreated (B) mandible after 16 weeks post-surgery from a representative pig are shown. Sections were stained with Sanderson's rapid bone stain and counterstained with van Gieson's picrofuchsin to stain mineralized tissue pink/red and soft tissue blue. Gutta-percha markers identifying the defect margins are also visible (pale peach circles). In both the autograft-treated and untreated sections, the border of the old bone (OB) and the new bone (NB) are visible in the high magnification images (border indicated with the yellow dashed line) and osteoblasts (indicated by arrows) can be seen in the lower panels. Blood vessels (BV) are present in the autograft-treated section.
Patricia L. Carlisle et al: Investigation of a pre-clinical mandibular bone notch defect model in miniature pigs: clinical computed tomography, micro-computed tomography, and histological evaluation. J Korean Assoc Oral Maxillofac Surg 2016

ment types over the duration of the experiment. Consistent with the CT analysis of the defect-superior ROI, the histological slides showed that bone invaded the marrow space superior to all defect sites, regardless of the treatment (apparent in Fig. 6 near the gutta-percha markers).

IV. Discussion

To ensure stringent pre-clinical evaluation of the healing capability of a novel bone regenerative biomaterial, ideally, the therapy is tested in a standardized CSD model. Due to the increasing reluctance to use companion animals for preclinical research and the stark differences between the masticatory biomechanics of sheep or goats and humans, CMF models in pigs have been favored. Pigs demonstrate similarity to human bone in form, function, bone healing characteristics, and bone mineral density[29]. Still, the consensus on defining what constitutes a full thickness notch type model in the pig mandible has been limited. Plug type bone defects ranging (diameter×depth) from 4×8 mm[33] to 9×4 mm[34] or 9×5 mm[35] or notch type defects ranging in size from 20×20 mm[36] to 20 ×10 mm[37] have all been evaluated in the minipig mandible. These observations have been primarily histological in nature with limited quantifiable metrics to demonstrate differences between the healing patterns of autologous grafts (positive controls) and sham treated (negative controls) groups. Spontaneous healing of the mandible post bone resection has also been clinically observed in patients[38-40]. This underlines the need for better characterization of healing patterns in the pig mandible models so that standardized interpretation of bone healing responses to novel bone graft materials is possible.

In the current study, we aimed to validate the premise that

a mandibular bone notch at least 6 cm^3 in volume in Sinclair miniature pigs can serve as a CSD. The presence of considerable bone in the untreated defect (average size in this study was 7.5 cm^3) at 16 weeks indicates that this model does not meet the criteria to be defined as a CSD. However, the absence of a significant healing response in either treatment group after 4 weeks suggests that this notch model could be used to investigate bone graft therapies that aim to accelerate the bone healing response. As a potential strategy to induce better bone regeneration by controlled mechanical stimulation, there is an increasingly greater emphasis on immediate implant placement and early loading[41]; techniques to accelerate new bone regeneration could prove critical to successful outcomes.

In this study, measurement of bone regeneration indicated that both autograft-treated and untreated mandibular defects had very similar bone healing profiles. Minimal mineralization had occurred in both the autograft-treated and the untreated notch defect sites over 4 weeks, followed by significant bone regeneration at 16 weeks. These observations suggest that, during the initial 4 week time period, the majority of the autograft was resorbed. Since histological analyses were not performed at 4 weeks, we cannot confirm if the autograft particles were undergoing fragmented remodeling, complete resorption, or only demineralization, each of which would have rendered them undetectable to clinical CT measurement. However, Jensen et al.[35] observed similar trends over 4 and 8 weeks using 1,000 to 2,000 μm range autologous bone chips to treat three-wall defects in the mandibular angles of Gottingen minipigs. The results of this study indicate that it is essential to include long-term evaluations of the healing response to biological bone graft particles in large animals. This may potentially apply to human treatments as well because bone regeneration and resorption of graft particles often proceed at varying rates.

An additional known factor that plays a role in graft bone healing success is size of the bone particles used. Pig bone particles in the range of 600 to 1,000 μm have been tested clinically as xenografts to treat maxillary sinus defects. At 5 months post-treatment with this particle size xenograft, researchers found retention of graft and significant new bone formation[42]. In the current study, we used a bone mill to create autologous bone graft chips that had an average size of 670 μm, which is within the range reported as ideal for bone graft preparation procedures[43].

While significant bone volume recovery was observed in the untreated defects and autologous graft treated groups after 16 weeks, there was very little structural maintenance of the original mandibular geometry. It has been previously reported that the bone in proximity of the injury site adapts and remodels to compensate for the weakness in the injury area[44]. Similar results were observed in this study, where the bone superior to the notch defect increased in volume, bulk, and thickness in 4 weeks and further in 16 weeks.(Fig. 3) This observed increase in volume with concurrent decrease in mineral density suggests that the mandible undergoes significant remodeling due to the creation of the notch defect in the mandible body and may be compensating for the loss of load carrying capacity. Similar to the loss of height and thickness in the alveolar ridge after the loss of dentition[45], this remodeling response in this model could be utilized when evaluating treatments attempting to maintain the original bone geometry, quality, and quantity necessary for implant restorations. It is critical for bone graft therapies to demonstrate not only on bone volume regeneration, but also maintenance of space and structure specific to the function of the CMF components.

V. Conclusion

A systematic standardized evaluation of a ~7.5 cm^3 mandibular bone notch defect model in the inferior margin of the miniature pig with periosteal resection was performed; autologous bone graft treatments were compared to untreated defects. Both experimental groups showed limited mineralized tissue within the defect site after 4 weeks, indicating that this model could be used to investigate therapies targeting accelerated bone regeneration at this early time point. However, the presence of significant bone within the defect site after 16 weeks in the untreated defect precludes the use of this model as a CSD for bone graft evaluation. In order to appropriately investigate bone graft materials, future studies should include appropriate negative controls in their choice of bone defect in the pig mandible to ensure lack of a significant spontaneous regenerative response.

Conflict of Interest

No potential conflict of interest relevant to this article was reported.

Acknowledgements

The authors would like to acknowledge Mr. James Herrick (Mayo Clinic) for his assistance with the histological analysis

and Dr. Tao You for assistance with the scanning electron microscopy.

This study has been conducted in compliance with the Animal Welfare Act, the implementing Animal Welfare Regulations, and the principles of the Guide for the Care and Use of Laboratory Animals.

The opinions or assertions contained herein are the private views of the author and are not to be construed as official or as reflecting the views of the Department of the Army or the Department of Defense.

ORCID

Patricia L. Carlisle, *http://orcid.org/0000-0001-6781-017X*
Teja Guda, *http://orcid.org/0000-0002-3218-2916*
David T. Silliman, *http://orcid.org/0000-0001-6440-4694*
Wen Lien, *http://orcid.org/0000-0001-5657-4765*
Robert G. Hale, *http://orcid.org/0000-0002-9699-3224*
Pamela R. Brown Baer, *http://orcid.org/0000-0001-6964-1955*

References

1. Mitchener TA, Canham-Chervak M. Oral-maxillofacial injury surveillance in the Department of Defense, 1996-2005. Am J Prev Med 2010;38(1 Suppl):S86-93.
2. Lew TA, Walker JA, Wenke JC, Blackbourne LH, Hale RG. Characterization of craniomaxillofacial battle injuries sustained by United States service members in the current conflicts of Iraq and Afghanistan. J Oral Maxillofac Surg 2010;68:3-7.
3. Owens BD, Kragh JF Jr, Wenke JC, Macaitis J, Wade CE, Holcomb JB. Combat wounds in operation Iraqi freedom and operation enduring freedom. J Trauma 2008;64:295-9.
4. Rachmiel A, Srouji S, Peled M. Alveolar ridge augmentation by distraction osteogenesis. Int J Oral Maxillofac Surg 2001;30:510-7.
5. Petrovic V, Zivkovic P, Petrovic D, Stefanovic V. Craniofacial bone tissue engineering. Oral Surg Oral Med Oral Pathol Oral Radiol 2012;114:e1-9.
6. Brown Baer PR, Wenke JC, Thomas SJ, Hale CR. Investigation of severe craniomaxillofacial battle injuries sustained by u.s. Service members: a case series. Craniomaxillofac Trauma Reconstr 2012;5: 243-52.
7. Bahat O, Fontanesi RV, Preston J. Reconstruction of the hard and soft tissues for optimal placement of osseointegrated implants. Int J Periodontics Restorative Dent 1993;13:255-75.
8. Lekholm U, Zarb GA. Patient selection and preparation. In: Brånemark PI, Zarb GA, Albrektsson T, eds. Tissue-integrated prostheses: osseointegration in clinical dentistry. Chicago: Quintessence Publishing; 1985:199-209.
9. Nasser M, Pandis N, Fleming PS, Fedorowicz Z, Ellis E, Ali K. Interventions for the management of mandibular fractures. Cochrane Database Syst Rev 2013;7:CD006087.
10. Zakhary IE, El-Mekkawi HA, Elsalanty ME. Alveolar ridge augmentation for implant fixation: status review. Oral Surg Oral Med Oral Pathol Oral Radiol 2012;114(5 Suppl):S179-89.
11. Reichert JC, Saifzadeh S, Wullschleger ME, Epari DR, Schütz MA, Duda GN, et al. The challenge of establishing preclinical models for segmental bone defect research. Biomaterials 2009;30:2149-63.
12. Fennis JP, Stoelinga PJ, Jansen JA. Mandibular reconstruction: a clinical and radiographic animal study on the use of autogenous scaffolds and platelet-rich plasma. Int J Oral Maxillofac Surg 2002;31:281-6.
13. Fennis JP, Stoelinga PJ, Jansen JA. Mandibular reconstruction: a histological and histomorphometric study on the use of autogenous scaffolds, particulate cortico-cancellous bone grafts and platelet rich plasma in goats. Int J Oral Maxillofac Surg 2004;33:48-55.
14. Fennis JP, Stoelinga PJ, Jansen JA. Reconstruction of the mandible with an autogenous irradiated cortical scaffold, autogenous corticocancellous bone-graft and autogenous platelet-rich-plasma: an animal experiment. Int J Oral Maxillofac Surg 2005;34:158-66.
15. Salmon R, Duncan W. Determination of the critical size for non-healing defects in the mandibular bone of sheep. Part 1: a pilot study. J N Z Soc Periodontol 1997;(81):6-15.
16. Marshall J, Duncan W. Determination of the critical size for non-healing defects in the mandibular bone of sheep. Part 2: healing of 12 mm circular defects after 16 weeks. J N Z Soc Periodontol 1997;(82):6-10.
17. Ayoub A, Challa SR, Abu-Serriah M, McMahon J, Moos K, Creanor S, et al. Use of a composite pedicled muscle flap and rh-BMP-7 for mandibular reconstruction. Int J Oral Maxillofac Surg 2007;36:1183-92.
18. Abu-Serriah M, Kontaxis A, Ayoub A, Harrison J, Odell E, Barbenel J. Mechanical evaluation of mandibular defects reconstructed using osteogenic protein-1 (rhOP-1) in a sheep model: a critical analysis. Int J Oral Maxillofac Surg 2005;34:287-93.
19. Abu-Serriah MM, Odell E, Lock C, Gillar A, Ayoub AF, Fleming RH. Histological assessment of bioengineered new bone in repairing osteoperiosteal mandibular defects in sheep using recombinant human bone morphogenetic protein-7. Br J Oral Maxillofac Surg 2004;42:410-8.
20. Gerard D, Carlson ER, Gotcher JE, Jacobs M. Effects of platelet-rich plasma on the healing of autologous bone grafted mandibular defects in dogs. J Oral Maxillofac Surg 2006;64:443-51.
21. Gerard D, Carlson ER, Gotcher JE, Jacobs M. Effects of platelet-rich plasma at the cellular level on healing of autologous bone-grafted mandibular defects in dogs. J Oral Maxillofac Surg 2007;65:721-7.
22. Messora MR, Nagata MJ, Pola NM, de Campos N, Fucini SE, Furlaneto FA. Effect of platelet-rich plasma on bone healing of fresh frozen bone allograft in mandibular defects: a histomorphometric study in dogs. Clin Oral Implants Res 2013;24:1347-53.
23. Hollinger JO, Kleinschmidt JC. The critical size defect as an experimental model to test bone repair materials. J Craniofac Surg 1990;1:60-8.
24. Pearce AI, Richards RG, Milz S, Schneider E, Pearce SG. Animal models for implant biomaterial research in bone: a review. Eur Cell Mater 2007;13:1-10.
25. Wang S, Liu Y, Fang D, Shi S. The miniature pig: a useful large animal model for dental and orofacial research. Oral Dis 2007;13:530-7.
26. Jeong HR, Hwang JH, Lee JK. Effectiveness of autogenous tooth bone used as a graft material for regeneration of bone in miniature pig. J Korean Assoc Oral Maxillofac Surg 2011;37:375-9.
27. Henkel KO, Gerber T, Dietrich W, Bienengräber V. Novel calcium phosphate formula for filling bone defects. Initial in vivo long-term results. Mund Kiefer Gesichtschir 2004;8:277-81.
28. Henkel KO, Gerber T, Lenz S, Gundlach KK, Bienengräber V. Macroscopical, histological, and morphometric studies of porous bone-replacement materials in minipigs 8 months after implantation. Oral Surg Oral Med Oral Pathol Oral Radiol Endod 2006;102: 606-13.
29. Ruehe B, Niehues S, Heberer S, Nelson K. Miniature pigs as an animal model for implant research: bone regeneration in critical-size defects. Oral Surg Oral Med Oral Pathol Oral Radiol Endod 2009;108:699-706.

30. Ma JL, Pan JL, Tan BS, Cui FZ. Determination of critical size defect of minipig mandible. J Tissue Eng Regen Med 2009;3:615-22.
31. Schneider CA, Rasband WS, Eliceiri KW. NIH Image to ImageJ: 25 years of image analysis. Nat Methods 2012;9:671-5.
32. Otsu N. A threshold selection method from gray-level histograms. Automatica 1975;11:23-7.
33. Strietzel FP, Khongkhunthian P, Khattiya R, Patchanee P, Reichart PA. Healing pattern of bone defects covered by different membrane types--a histologic study in the porcine mandible. J Biomed Mater Res B Appl Biomater 2006;78:35-46.
34. Jensen SS, Bornstein MM, Dard M, Bosshardt DD, Buser D. Comparative study of biphasic calcium phosphates with different HA/TCP ratios in mandibular bone defects: a long-term histomorphometric study in minipigs. J Biomed Mater Res B Appl Biomater 2009;90:171-81.
35. Jensen SS, Broggini N, Hjørting-Hansen E, Schenk R, Buser D. Bone healing and graft resorption of autograft, anorganic bovine bone and beta-tricalcium phosphate: a histologic and histomorphometric study in the mandibles of minipigs. Clin Oral Implants Res 2006;17:237-43.
36. Abukawa H, Shin M, Williams WB, Vacanti JP, Kaban LB, Troulis MJ. Reconstruction of mandibular defects with autologous tissue-engineered bone. J Oral Maxillofac Surg 2004;62:601-6.
37. Gröger A, Kläring S, Merten HA, Holste J, Kaps C, Sittinger M. Tissue engineering of bone for mandibular augmentation in immunocompetent minipigs: preliminary study. Scand J Plast Reconstr Surg Hand Surg 2003;37:129-33.
38. Coen Pramono D. Spontaneous bone regeneration after mandible resection in a case of ameloblastoma: a case report. Ann Acad Med Singapore 2004;33(4 Suppl):59-62.
39. Ihan Hren N, Miljavec M. Spontaneous bone healing of the large bone defects in the mandible. Int J Oral Maxillofac Surg 2008;37:1111-6.
40. Ogunlewe MO, Akinwande JA, Ladeinde AL, Adeyemo WL. Spontaneous regeneration of whole mandible after total mandibulectomy in a sickle cell patient. J Oral Maxillofac Surg 2006;64:981-4.
41. Zambon R, Mardas N, Horvath A, Petrie A, Dard M, Donos N. The effect of loading in regenerated bone in dehiscence defects following a combined approach of bone grafting and GBR. Clin Oral Implants Res 2012;23:591-601.
42. Orsini G, Scarano A, Piattelli M, Piccirilli M, Caputi S, Piattelli A. Histologic and ultrastructural analysis of regenerated bone in maxillary sinus augmentation using a porcine bone-derived biomaterial. J Periodontol 2006;77:1984-90.
43. Miron RJ, Gruber R, Hedbom E, Saulacic N, Zhang Y, Sculean A, et al. Impact of bone harvesting techniques on cell viability and the release of growth factors of autografts. Clin Implant Dent Relat Res 2013;15:481-9.
44. Liu W, Tang XJ, Zhang ZY, Yin L, Gui L. 3D-CT evaluation of mandibular morphology after mandibular outer cortex osteotomy in young miniature pigs: the role of the periosteum. J Craniomaxillofac Surg 2014;42:763-71.
45. Van der Weijden F, Dell'Acqua F, Slot DE. Alveolar bone dimensional changes of post-extraction sockets in humans: a systematic review. J Clin Periodontol 2009;36:1048-58.